Astron. Astrophys. 351, 1028–1035 (1999)

ASTRONOMY AND ASTROPHYSICS

Gravity dependence at the bottom of the main sequence

Serena Viti[1] **and Hugh R.A. Jones**[2]

[1] Department of Physics and Astronomy, University College London, London WC1E 6BT, UK
[2] Astrophysics Research Institute, Liverpool John Moores University, Twelve Quays House, Egerton Wharf, Birkenhead CH41 1LD, UK

Received 9 July 1999 / Accepted 1 October 1999

Abstract. We investigate the effects of gravity on the infrared spectra of objects around the M dwarf to brown dwarf transition. We focus on observations of the very low-mass objects TVLM 513–46546 and GJ 569B from 1 to 2.5 μm. These objects have very similar spectral types and colours but they differ by more than a magnitude in luminosity; this indicates that their surface gravities differ by around 0.5 dex. We compare their spectra and present line identifications in the infrared. We investigate at low resolution the sensitivity of some of the atomic features to changes in surface gravities and make comparisons with recent atmospheric models. We identify seven surface gravity sensitive features. We find that the difference in surface gravity between the spectra are consistent with GJ 569B having a lower surface gravity than TVLM by at least 0.5 dex which suggests GJ 569B is a brown dwarf. Because of the relatively few surface gravity features which can be identified at low resolution, confirmation of this result should be made with observations at higher resolution which would enable more gravity sensitive features to be identified with better precision.

Key words: stars: atmospheres – stars: fundamental parameters – stars: low-mass, brown dwarfs

1. Introduction

By number density, low mass stars (LMS) are the dominant objects in our Galaxy. Because of the complexity of their spectra, which are dominated by water in the infrared and titanium oxide in the optical, standard techniques, such as blackbody curve fits, used for hotter stars to find essential parameters such as the bolometric luminosities and effective temperatures, are not applicable. The determination of LMS fundamental parameters such as the effective temperature, the metallicity and the age rely both on a direct empirical comparison among stars of similar spectral classes and on a careful fit to synthetic spectra.

Although the infrared spectra of late-type M dwarfs are strongly affected by the presence of water bands, many atomic features can be resolved by careful observations. Some of the atomic features have proved to be fairly sensitive to changes in effective temperature and metallicity (Jones et al. 1996, Viti et al. 1997). We still lack, however, any direct measurements for the age of LMS. Age becomes an increasingly important parameter towards lower masses. For example a 0.2 $M_\odot$ object takes 0.2 Gyr to reach the main sequence, a 0.1 $M_\odot$ object takes 1 Gyr whereas a 0.075 $M_\odot$ object takes 2.5 Gyr (e.g. see Fig. 1). A reliable measure of age for LMS is therefore vital for locating them on a Hertzsprung-Russell diagram. As with effective temperature and metallicity, surface gravity is also sensitive to age. If we can measure surface gravity accurately we can in principle distinguish between young cooling brown dwarfs and old late–type M dwarfs with similar colours. For example, Fig. 6 in Burrows et al. (1993) shows that at the bottom of the main sequence objects with mass of ~ 0.01 $M_\odot$ (brown dwarfs) have a much lower surface gravity than late M dwarfs (~ 0.2 $M_\odot$) even at late times.

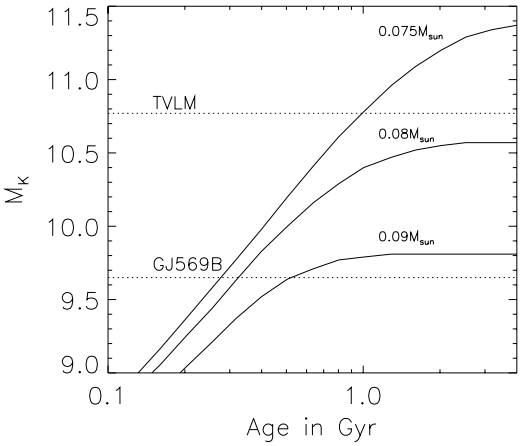

Fig. 1. Absolute K magnitude versus age at the bottom of the main sequence (Burrows et al. 1997). The dotted lines represent the magnitudes for TVLM and GJ 569B compared to expectations based on models (solid) of 0.075, 0.08 and 0.09 solar masses.

2. The targets

We analyse 1.0–2.5 μm spectra from two well observed late-type dwarfs, TVLM 513-46546 (hereafter TVLM) and GJ 569B. The objects have similar colours and the same spectral type of M8.5V; they were placed next to one another in the standard

Send offprint requests to: S. Viti (sv@star.ucl.ac.uk)

Table 1. Observational data for GJ 569B and TVLM. For TVLM the values are from the following sources: photometry from Tinney et al. (1995), Leggett et al. (1998); space velocities from Tinney & Reid (1998); distance from Tinney et al. (1995). For GJ 569B the values are from the following sources: photometry from Forest et al. (1988) and Becklin & Zuckerman (1988); distance from Perryman et al. (1997), this is for GJ 569A; space velocities from Marcy et al. (1987), these are for GJ 569A. The I-band photometry for GJ 569B is given in brackets since it was determined 'in thick and variable cloud cover' (Forest et al. 1988). Errors in distance are given in brackets.

	Spectral Type	M_K	J–L'	I	J	H	K	L'	d pc	U,V,W km s^{-1}
TVLM513-46546	M8.5	10.77	1.77	15.09	11.80	11.12	10.72	10.03	9.92 (0.23)	–4.0,–12.5,1.5
GJ 569B	M8.5	9.60	1.85	(13.88)	10.78	10.11	9.60	8.85	9.81 (0.16)	–10,4,-15

Table 2. Central wavelength ($\lambda_{\rm cen}$), resolution ($\Delta\lambda$), dates of the observations and integration times.

Object	$\lambda_{\rm cen}$ (μm)	$\Delta\lambda$ (μm)	Date	Exp. Time (total) minutes
TVLM 513–4546	1.135	0.00044	16/05/95	30
	1.415	0.00044	16/05/95	20
	1.635	0.00044	16/05/95	25
	2.070	0.00088	16/05/95	30
GJ 569B	1.135	0.00044	12/05/95	15
	1.415	0.00044	16/05/95	20
	1.635	0.00044	16/05/95	12
	2.070	0.00088	16/05/95	10

Table 3. List of surface gravity sensitive features found in the grid of models considered. The wavelengths with a * highlight features which also show gravity sensitivity among higher temperatures models. Wavelengths given to three significant figures instead of four indicate regions or features where molecular opacities are of particular importance. The region 1.5–1.6 μm is especially affected by water opacities.

λ	Element	λ	Element	λ	Element	λ	Element
1.0066	Ti	1.2944	Al	1.1060	Al	1.5872	Si
1.0074	Ti	1.2949	Al	1.1082	Al	1.5878	Si
1.0102	Ca	1.2954	Al	1.1092	Fe	1.6004*	Ca
1.0107	Ca	1.3168	Al	1.1100	Fe	1.603*	Ca
1.0112	Ca	1.3178	Al	1.1107	Fe	1.627*	Ca
1.0122	Ca	1.3202*	Al	1.1118	Fe	1.6302	Ca
1.0134	Ca	1.3234	Al	1.1162	Cr	1.6342	Ca
1.0138	Ca	1.541	Ti/Mg	1.1160	Cr	1.6510	Fe
1.0142	Ca	1.542	Mg	1.1192*	Ni	1.661	Al
1.0157	Fe	1.553*	Ti	1.1200	Ni	1.672*	Al
1.0162	Fe	1.554*	Ti	1.1562	Fe	1.6781*	Al
1.0170	Fe	1.5568	Ti	1.1617	Fe	1.6857*	Al
1.0184	Ti	1.5604*	Ti	1.1876*	Fe	1.7114*	Mg
1.0193	Ti	1.5732	Mg	1.2068*	Mg	1.7136	Mg
1.0210	Ti	1.5760	Mg	1.2486	Ti	2.0226*	Ca
1.0216	Fe	1.5768	Mg	1.2494	K	2.0406	Mg
1.0317	Ti	1.5788	Mg	1.2607	Ti	2.0593	Mg
1.0838	Na	1.5797	Mg	1.2619–1.2684*	Na	2.0789*	Mg
1.0908*	Cr	1.580	Mg	1.2736	Ti	2.1028	Al
1.0915*	Cr	1.5808	Mg	1.2758–1.2788	Ca	2.1783	Ti
1.0920*	Cr	1.5836	Mg	1.2874	Mn	2.227	Ti
1.0935*	Si	1.5862*	Mg	1.2912	Mn	2.2432	Fe/Ti

spectral sequence of Kirkpatrick et al. (1995). This means that they have a very similar temperature. Their space velocities indicate they are young although they have substantially different luminosities. This could be an effect due to a difference in age. Fig. 1 illustrates how the targets observed luminosities relate to theoretical models. We investigate this hypothesis by looking for differences in their surface gravities. Table 1 details some of the known fundamental parameters for our targets TVLM and GJ 569B.

2.1. TVLM 513–46546

TVLM is a very low-mass M dwarf discovered by Tinney et al. (1993) in a survey of 270 square degrees of Schmidt plates.

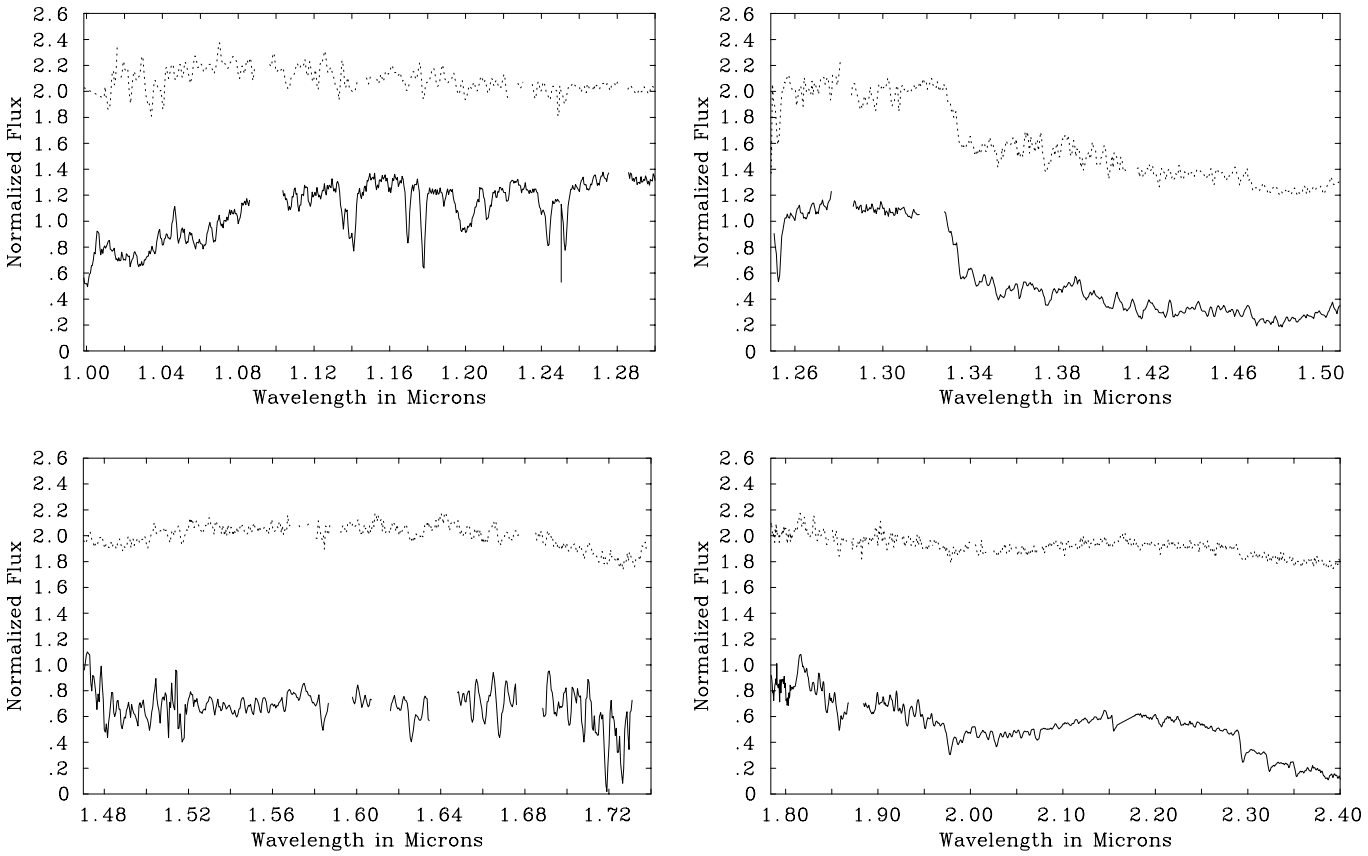

Fig. 2. Spectra of GJ 569B (upper) and TVLM (lower) at the four grating positions observed. Some 'gaps' due to the removal of hydrogen lines or to overlapping of grating positions (see text) are not present in both the stars; this is due to the use of two different standards.

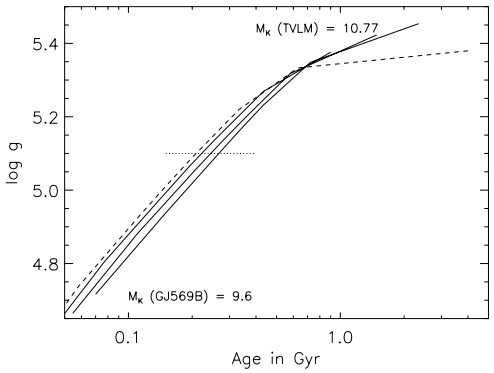

Fig. 3. Surface gravity versus age for constant temperature isochrones from Burrows et al. (1997). Temperatures of 2200, 2350, 2500 K are shown as solid lines. The position of the labels for M_K (GJ 569B) and M_K (TVLM) are appropriate to their place in the diagram. For example, the solid line ending directly beneath 10.77 in the top right of the diagram corresponds to a 2350 K model with an age 1.48 Gyr, M_K = 10.73 and log g = 5.42; this solid line is terminated at this point because higher log g's and older ages would yield too large values to fit within the observed M_K's. The line for 2600 K is shown as a dashed line because models of this temperature never reach low enough M_K to fit with the observed value for TVLM. The dotted line is the limit set by the non–detection of lithium (Magazzu et al. 1993), however, the lack of signal–to–noise of this result means that it is not actually a hard limit on the gravity of GJ 569B.

Table 4. Infrared spectral features sensitive to surface gravity changes. In the first and second column we list the feature with its central wavelength; the third column indicates the star where the feature is stronger; the fourth column indicates if the features increase (Up–arrow) or decreases (Down–arrow) with the increasing of surface gravity.

Line	λ	star	log g
Mg	1.206	GJ 569B	$\Downarrow$
Ti	1.260	GJ 569B	$\Downarrow$
Na	1.263	GJ 569B	$\Downarrow$
Mn	1.291	GJ 569B	$\Downarrow$
Al	1.294	GJ 569B	$\Downarrow$
Mg	1.711	GJ 569B	$\Downarrow$
Mg	1.713	GJ 569B	$\Downarrow$

Its photometric colours and parallax (Tinney et al. 1995) place it at the bottom of the main sequence (see figures in Leggett et al. 1998). From its position in Fig. 6 of Leggett et al. and its low space velocity and tangential velocity (Tinney & Reid 1998) it fits with our expectations for a very low-mass young-disk object. The lack of lithium in its spectrum and the lithium burning limit (e.g. Magazzu et al. 1993) constrain it to be more massive than 0.06 $M_\odot$.

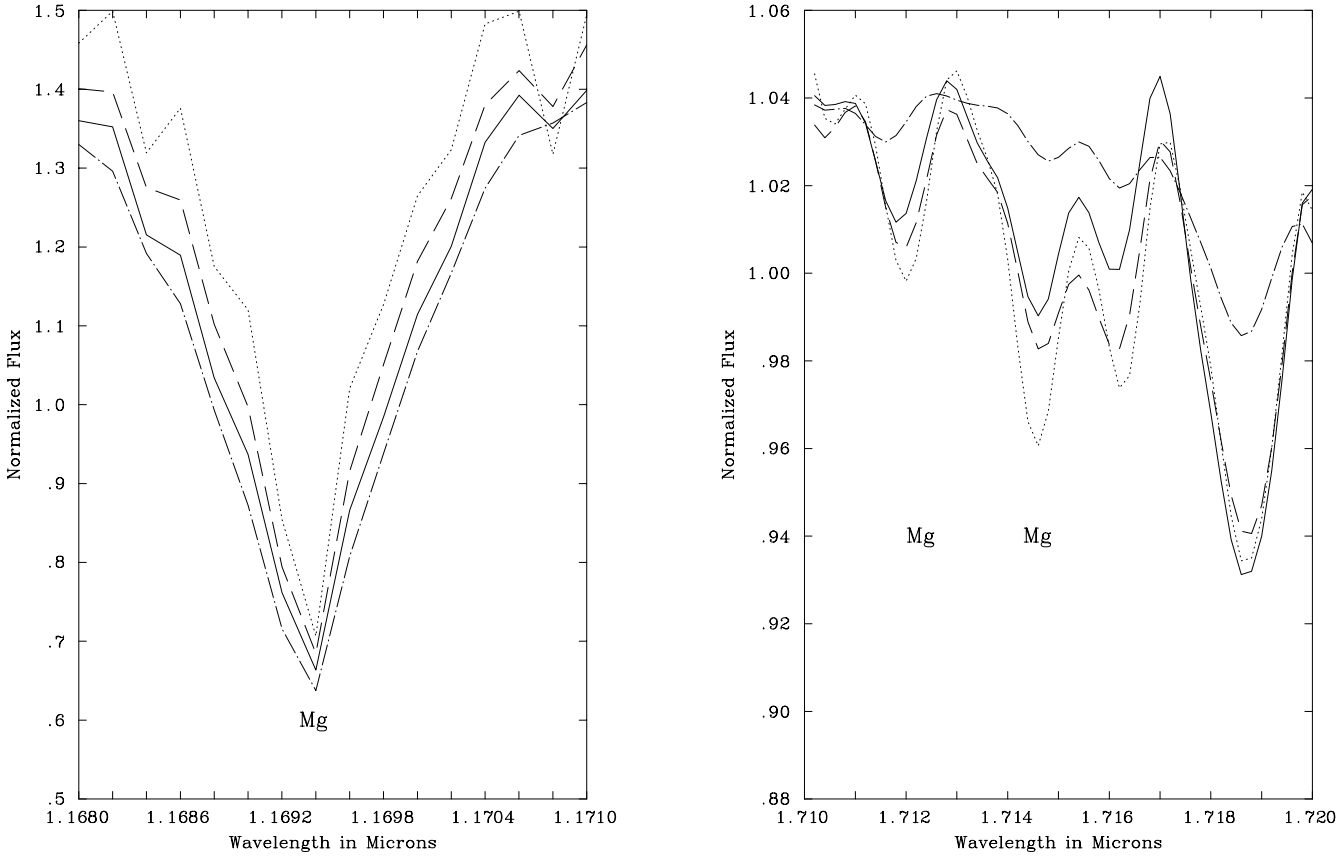

Fig. 4. Sensitivity of models to changes in effective temperature, metallicity and surface gravity. Left panel: magnesium feature where differences between models produce similar changes for an increase in surface gravity (· · · to —), an increase in effective temperature (— to .-.) and a decrease in metallicity (— to - - -). Right panel: magnesium features showing a larger sensitivity to surface gravity and effective temperature and then to metallicity. In both plots: $T_{\rm eff}$ = 2400 K, log g = 5.5, [M/H] = 0.0 is plotted with a continuous line, $T_{\rm eff}$ = 2500 K, log g = 5.5, [M/H] = 0.0 with a dot–dash line, $T_{\rm eff}$ = 2400 K, log g = 5.0, [M/H] = 0.0 with a dotted line and $T_{\rm eff}$ = 2400 K, log g = 5.5, [M/H] = -0.5 with a dashed line.

2.2. GJ 569B

Discovered in 1988 about 5 arcsec from a dM2e star, Forest et al. (1988) showed GJ 569B to have a common proper motion with its companion. The primary star has emission lines, a low space velocity and exhibits flaring. These characteristics indicate youth for the system and thus GJ 569B's low luminosity and red colours make it a candidate to be a young cooling brown dwarf. The lack of lithium in GJ 569Bs' spectrum constrains it to be more massive than 0.06 $M_{\odot}$ (Magazzu et al. 1993). Henry & Kirkpatrick (1990) noted that the H alpha emission of GJ 569A is consistent with a Hyades age ($\sim$ 0.5 Gyr) and marginally consistent with the age of the Pleiades ($\sim$ 0.1 Gyr). From the HIPPARCOS–determined distance (to GJ 569A, Perryman et al. 1997), we estimate that GJ 569B is overluminous by $\sim$ 0.65 mag with respect to stars with the same colours and spectral type (Jones et al. 1996).

3. Observations and data reduction

GJ 569B and TVLM were observed, among other M dwarfs (Viti et al. 1997), on the nights of 1995 May 12 and 16 during the commissioning of the upgraded Cooled Grating Spectrometer 4 (CGS4, Puxley et al. 1992) on the UK Infrared Telescope (UKIRT) on Mauna Kea, Hawaii. CGS4 uses a 256 x 256 InSb array. Comparison sky spectra were obtained by nodding the telescope so that the object was measured successively in two rows of the array, separated by 30 arcsec. We aimed to observe throughout the three near infrared bands J, H and K. The 75 line mm^{-1} grating was used with central grating wavelengths of 1.135, 1.415, 1.635 and 2.070 μm. The coverage, resolution and integration times of the observations are listed in Table 2. Most grating positions overlap with the previous and the next at the two ends thus ensuring reliable coverage of the whole region. To remove telluric bands of water, oxygen, carbon dioxide and methane, we chose the following standards: (i) SAO101293 and BS5633 for GJ 569B which have the spectral type A0 with V = 5.77 and an A3 with V = 6.02; (ii) SAO101879 for TVLM which is an A0 with V = 6.00. The choice of those standards was based on the expectation that such stars have no features in common with M dwarfs and are featureless in the infrared except for some hydrogen lines.

The observations were made during excellent conditions (optical seeing $\sim$ 1 arcsec and low atmospheric humidity $\sim$ 20

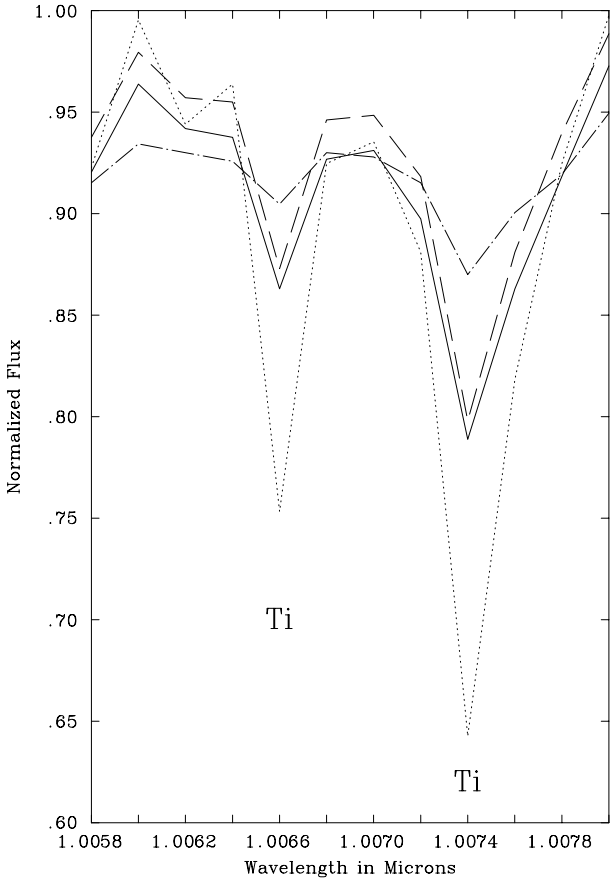

Fig. 5. Two titanium surface gravity sensitive features. T_{eff} = 2400 K, log g = 5.5, [M/H] = 0.0 is plotted with a continuous line, T_{eff} = 2500 K, log g = 5.5, [M/H] = 0.0 with a dot–dash line, T_{eff} = 2400 K, log g = 5.0, [M/H] = 0.0 with a dotted line and T_{eff} = 2400 K, log g = 5.5, [M/H] = -0.5 with a dashed line.

per cent). The airmass difference between object and standard never exceeded 0.05 and so we are confident that the spectra have good cancellation of atmospheric features. Some of the hydrogen lines introduced into the spectrum when dividing by the standard had, however, to be removed manually. Gaps in the final spectrum represent (i) regions where hydrogen emission lines were manually removed and (ii) regions where the end of a grating position did not overlap with the next one (see Fig. 2). Both the objects and the standards were wavelength calibrated by using arc lines of krypton, argon and xenon. The accuracy of the calibration is around 0.5×10^{-3} μm. The sky subtraction was obtained with standard routines which eliminate any residual sky emission due to the variance of sky brightness between object and sky pairs. The signal was spread between three rows. To extract the spectrum from the sky subtracted signal an Optimal Extraction technique was used; this combines the rows using weights based on the spatial profile of the stellar image. These procedures were followed partly by using software provided for CGS4 data and by using the *Figaro*, *Specdre* and *Kappa*, packages provided and supported by Starlink.

Due to the relatively close separation of the components of GJ 569AB, the spectra of GJ 569B were partially contaminated by the primary component, GJ 569A. As expected, the contamination was wavelength dependent and strongest in the J band. The contamination was removed by (i) estimating the contribution of GJ 569A in the rows symmetrically opposite to the rows where GJ 569B was centred at, (ii) subtracting this contamination from the GJ 569B. We found the error in making this correction to be typically 3% of the contamination. The contamination itself was also relatively small: 30% contamination at 1.135 μm; 9% at 1.415 μm; 5% at 1.635 μm and 2% at 2.070 μm.

4. Spectral analysis

We have measured the overluminosity of GJ 569B with respect to TVLM by directly integrating the absolute flux of the infrared spectra of the two stars and we find it to be almost twice as luminous as TVLM in accord with the expected overluminosity of GJ 569B based on its photometry. Fig. 2 shows the observational data plotted for the four grating positions. The spectra of the two stars have been normalized to have the same mean value at each grating position and a constant has been added to the flux of GJ 569B for clarity.

Viti et al. (1997) showed that we can infer effective temperature and to a lesser extent metallicity by a detailed analysis of spectral features in the optical and infrared. Grids of models computed at different values of effective temperature and metallicity show how sensitive some spectral features are to these parameters (Jones et al. 1996; Viti et al. 1997). Surface gravity however shows less sensitivity (Jones et al. 1996). The aim of this work is to identify spectral features which are particularly sensitive to surface gravity changes and mostly insensitive to effective temperature and metallicity changes. To find such spectral features we use a grid of NextGen models by Allard et al. (1997): we have examined a subset of models ranging in surface gravity from log g = 4.5 to 5.5, in metallicity from [M/H] = -0.5 to 0.0 and in effective temperature from T_{eff} = 2400 to 2700 K.

We have concentrated on the intercomparison of four models with the most appropriate parameters from the grid:

Model 1: T_{eff} = 2400, log g = 5.5, [M/H] = 0.0
Model 2: T_{eff} = 2500, log g = 5.5, [M/H] = 0.0
Model 3: T_{eff} = 2400, log g = 5.0, [M/H] = 0.0
Model 4: T_{eff} = 2400, log g = 5.5, [M/H] = -0.5.

The base temperature of 2400 K is chosen to be in accordance with both the 'observationally' and 'theoretically' determined values in Jones et al. (1996). We note that a temperature much lower than 2400 K together with the non-detection of lithium in GJ 569B would imply a relatively smaller radius and therefore a lower absolute magnitude for GJ 569B. We have considered 100 K differences in effective temperature although it is unlikely that the two objects differ by more than 50 K. In a paper on spectral typing for late-type M dwarfs (Kirkpatrick et al. 1995), GJ 569B and TVLM lie next to one another with a spectral type of a M8.5V in a spectral sequence from M7 to M9.5. In this sequence ten objects separate the well observed objects VB10 (earliest M8) and LHS2924 (latest M9). The assignment of ab-

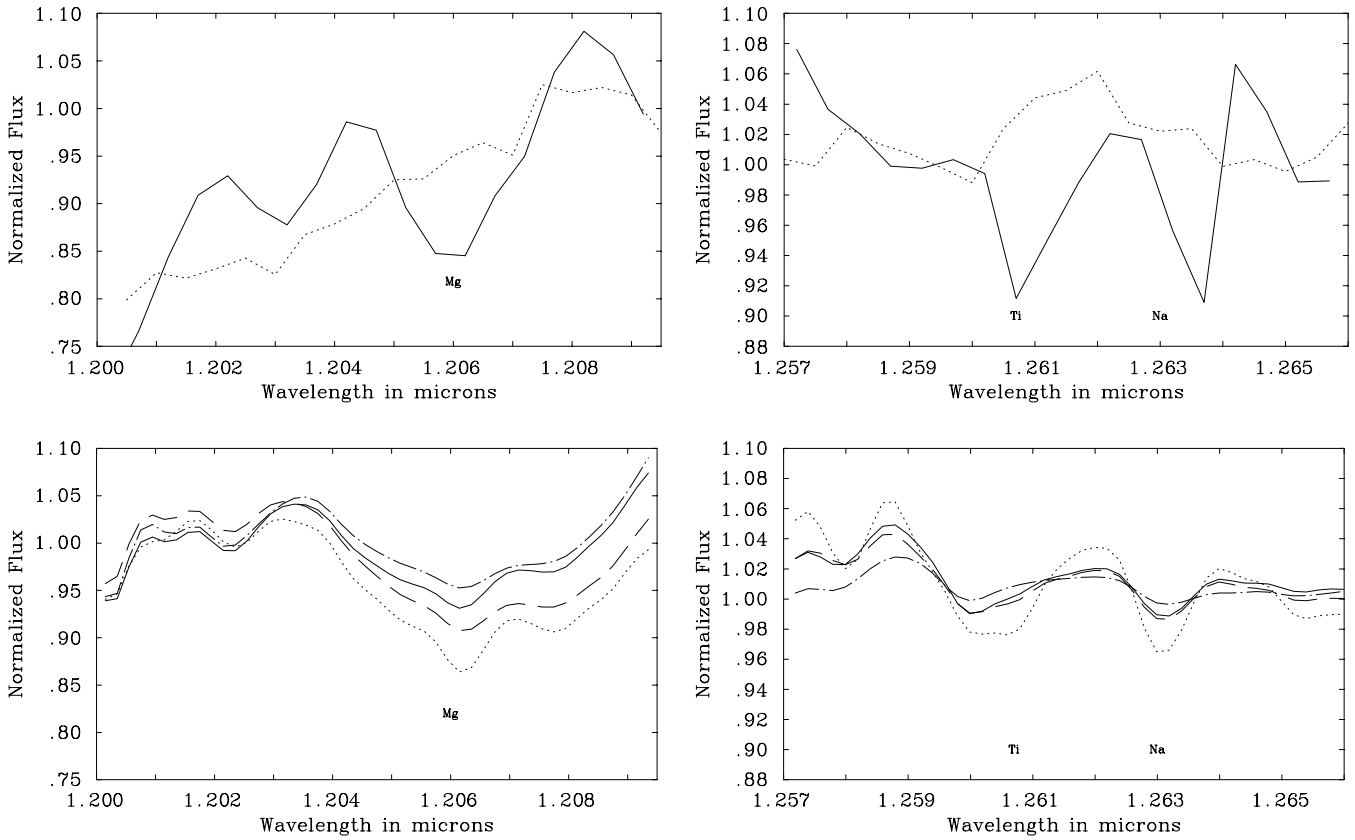

Fig. 6. Top panels: GJ 569B (continuous line) and TVLM (dotted line) overplotted for two chosen features. Bottom panels: same regions as top panels but for the synthetic spectra. As for Fig. 4, continuous line corresponds to T_{eff} = 2400 K, log g = 5.5, [M/H] = 0.0 model while, dot–dash line corresponds to T_{eff} = 2500 K, log g = 5.5, [M/H] = 0.0, dotted line to T_{eff} = 2400 K, log g = 5.0, [M/H] = 0.0 and dot dot dash line to T_{eff} = 2400 K, log g = 5.5, [M/H] = -0.5.

solute temperatures to late-type M dwarf spectral types has led to a wide range of values in the literature. Although older work has found VB10 and LHS2924 to differ in effective temperature by 250–290 K (Berriman et al. 1992; Tinney et al. 1993; Kirkpatrick et al. 1993; Jones et al. 1994) an improved analysis and new models by Tsuji et al. (1996) indicate that the difference is only around 120–140 K. If the ten objects intermediate in spectral type between VB10 and LHS2924 are evenly spaced then objects next to one another, TVLM and GJ 569B, should differ by 10(–30) K depending on the adopted temperature scale.

From the analysis of solar neighbourhood stars by Edvardsson et al. (1993), using data of K and M dwarfs kinematical properties from Wielen (1977), the scatter in metallicity in the solar neighbourhood for ages of 1 Gyr is around 0.1 dex (see Fig. 31 and Table 15 from Edvardsson et al. 1993), therefore our choice of looking at metallicity differences of -0.5 dex is also rather conservative. Our choice of surface gravities is based on Fig. 3 where we note that the range of allowed surface gravities may be a little larger than the 0.5 differences plotted. This means that for GJ 569B and TVLM, the relatively large differences between our chosen models parameters and those expected for the targets are likely to overemphasize the importance of temperature and metallicity compared to differences in surface gravity.

4.1. Surface gravities

Infrared spectra of late–type M dwarfs are relatively difficult to analyse due to the absence of a continuum and the importance of molecular opacities together with the many atomic elements present at such low temperatures. Unsurprisingly we cannot find atomic features which are exclusively sensitive to surface gravity. They all show some dependence, weak or strong, on changes in effective temperature and metallicity. In general we find that gravity sensitivity of a feature is not metallicity dependent though it is temperature dependent. Our technique is to find those features which show a large difference between Model 1 and 3 (gravity changes) where Models 2 and 4 (temperature and metallicity changes respectively) are relatively closer to Model 1. By overplotting the models we found more than 50 features which are primarily sensitive to surface gravity, log g (see Table 3). Many of these features are too weak to be identified in our observed spectra. The identification from the model output is performed as follows: at every wavelength, the 'strongest' atomic and molecular line is identified. The lines identified in Table 3 as atomic may be 'blended' by stronger molecular opacity. The wavelengths of the lines most likely to be affected are given to fewer decimal places.

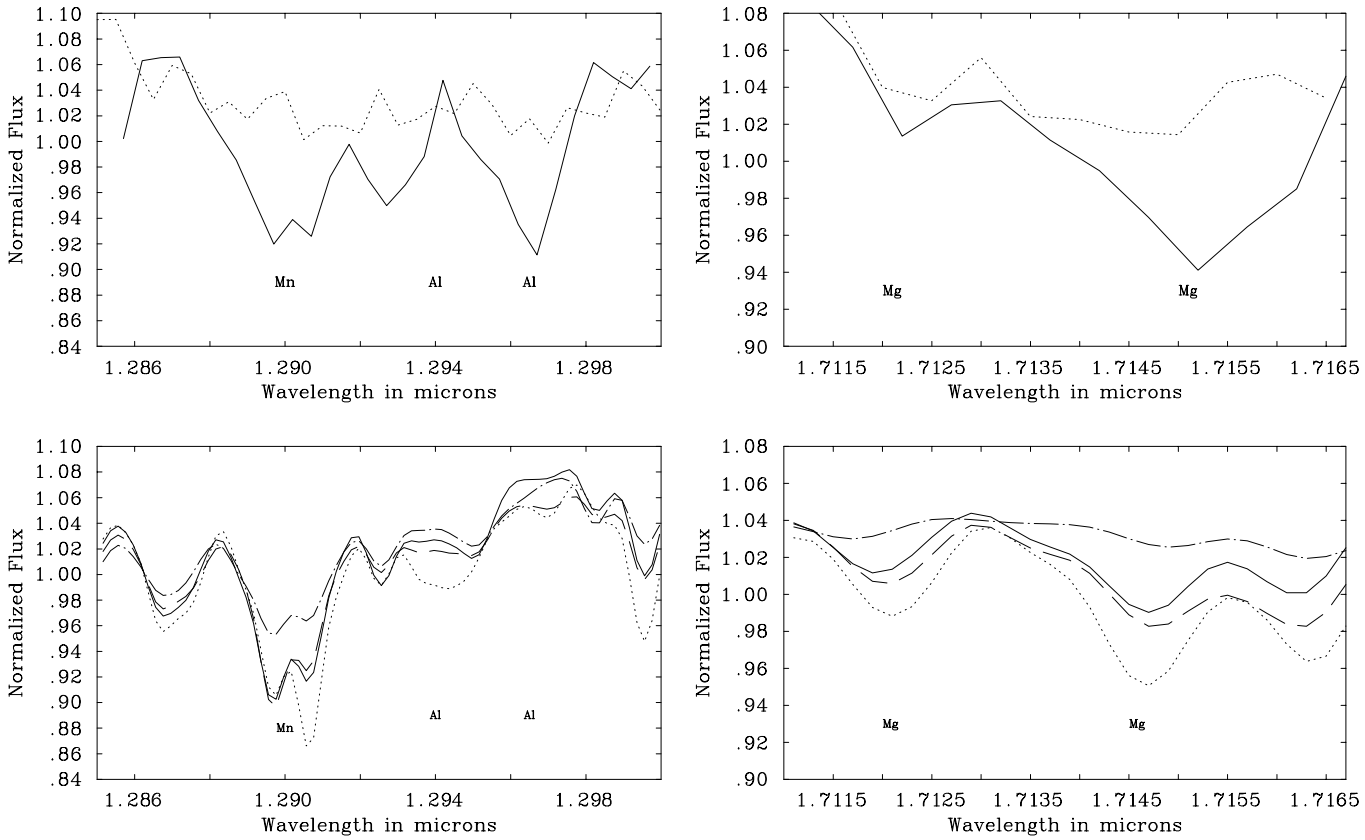

Fig. 7. As in Fig. 6 but for different wavelength regions.

Many of these features are also sensitive to effective temperature and/or metallicity changes but in such a way that, provided a reasonable sample of high resolution spectra is available, a pattern can be found. Some regions (1.35–1.55 μm and 1.72–2.00 μm) are not covered by Table 3 because they are too affected by molecular opacities (mainly water) and therefore dependent on small effective temperature changes. Surface gravity differences could be better spotted from the highest resolution spectra where the effects of blending are minimized. A resolution of 0.0002 μm would be sufficient to identify the features listed in Table 3. This is easily within the capability of modern echelle spectrometers, e.g, the resolving power of CGS4 echelle and long camera on UKIRT is up to 37000.

In Fig. 4 we overplot the four models across two different wavelength regions to represent sensitivities to surface gravity, effective temperature and metallicity. The right panel shows two synthetic magnesium features. These features are sensitive to both surface gravity and metallicity but the metallicity differences produce changes which are distinctively different to those produced by a surface gravity change. On the other hand the synthetic magnesium feature in the left panel shows less pronounced sensitivity to all the three parameters. Fig. 5 shows two of the best gravity sensitive features which are titanium around $\sim$ 1.007 μm. These are good examples of features which we could not use because of the relatively low resolution of our observations.

Figs. 6 and 7 show a line by line overplotting of the two stars and compare seven surface gravity sensitive features identifiable in our observed spectra. Below the observed spectra we plot the same region for the models to match those of the observations. All the features show consistency in the behaviour of surface gravity. In particular, we note that the magnesium feature at $\sim$ 1.206 μm and the aluminium bands centered at $\sim$ 1.295 μm can not be identified in the log g = 5.5 models when their resolution is lowered to match the one of the observations. This behaviour is consistent with the observations.

Table 4 lists the spectral features plotted.

The features indicate that GJ 569B has lower surface gravity than TVLM. However, we notice that the surface gravity differences between the two spectra relative to the models are substantially larger than the Δ0.4 dex or less that might be expected from comparisons of the theoretical models and the non-detection of lithium (see Fig. 3). One easy way to explain the apparent large gravity difference would be if the system GJ 569AB is young and thus GJ 569B's gravity is below the dotted line in Fig. 3. This requires discounting the evidence of age for the system: (1) the non–detection of lithium in the spectrum of GJ 569B and (2) the relative weak H alpha emission line seen in GJ 569A. The only strong constraint on the systems' age is that it is older than around 0.02 Gyr, otherwise GJ 569A would appear to be overluminous.

Another way to explain the differences in the spectra is the presence of different amount of dust in the atmospheres of our targets. The models used for this analysis do not include dust grains. Dust formation tends to make the atmosphere more transparent, and could be consistent with the differences observed between the two stars: deeper lines against a brighter continuum as TiO begins to condense away. Based on observations and preliminary models (e.g. Jones & Tsuji 1997, 1998, in preparation), however, dust formation in the photospheres of low-mass objects is predominately of small grain sizes. According to models and observations this means little effect can be seen at the relatively high temperatures (> 2200 K) in spectra longward of around 0.9 μm. This, together with the similar temperature of our targets suggests that dust should have little effect on these spectra. Nonetheless a dust explanation can not be ruled out until the effects of dust have been more fully investigated.

5. Conclusions

From Table 4, and Figs. 6 and 7 we find that GJ 569B has a lower surface gravity than TVLM by at least 0.5 dex. This gravity difference suggests that GJ 569B is younger than TVLM making it a likely brown dwarf and thus should be searched for lithium at higher signal to noise than previous observations have managed.

Our technique of looking for gravity differences between objects using gravity sensitive lines may be used to find the relative ages for stars at the end of the main sequence and for brown dwarfs. The potential sensitivity of this method to find the ages for low-mass objects lies in their slow cooling rates. The determination of such ages is essential to find the field object mass function into the brown dwarf regime.

This study was limited mainly by the lack of resolution in our observations. By comparison of synthetic spectra we have shown that even within the uncertainties of the models' parameters (molecular linelists, dust opacities, atomic oscillator strengths) there are some atomic features that are mainly sensitive to changes in surface gravity. In particular, there are some features (or bands) that show sensitivity to surface gravity at both low (2400 K) and high temperatures (2700 K) (see Table 3). Among them, the Mn feature at ~ 1.711 μm is identified in the low resolution spectra presented here.

We notice that gravity sensitivity is also evident in the synthetic optical part of the spectrum (e.g. Martin et al. 1999). However it is desirable to pursue the technique in the infrared where it can be much more easily applied to the brown dwarf regime.

Future work should concentrate on obtaining high resolution near IR spectra of GJ 569B and TVLM and use the latest available models to investigate their surface gravities. Ideally this work should also be carried out on low-mass eclipsing binary system with component masses spanning the low-mass star / brown dwarf transition and objects within clusters where the targets have a known age.

Acknowledgements. SV acknowledges the financial support of PPARC post–doctoral research assistantship. The authors thank Adam Burrows and Peter H Hauschildt for the use of their models and the referee for useful comments.

References

Allard F., Hauschildt P.H., Alexander D.R., Starrfield S., 1997, ARA&A 35, 137
Becklin E.E., Zuckerman B., 1988, Nat 336, 656
Berriman G., Reid N., Leggett S.K., 1992, ApJ 392, L31
Burrows A., Hubbard W.B., Saumon D., Lunine J.I., 1993, ApJ 406, 158
Burrows A., Marley M., Hubbard W.B., et al., 1997, ApJ 491, 856
Edvardsson B., Andersen J., Gustafsson B., et al., 1993, A&A 275, 101
Forest W.J., Shure M., Skrutskie M.F., 1988, ApJ 330, 119L
Henry T.J., Kirkpatrick J.D., 1990, ApJ 354, L29
Jones H.R.A., Tsuji T., 1997, ApJ 480, L39
Jones H.R.A., Tsuji T., 1998, In: Rebolo R., Martin E.L., Zapatero Osorio M. (eds.) Brown dwarfs and extrasolar planets. ASP Conference Series 134, p. 423
Jones H.R.A., Longmore A.J., Jameson R.F., Mountain C.M., 1994, MNRAS 267, 413
Jones H.R.A., Longmore A.J., Allard F., Hauschildt P.H., 1996, MNRAS 280, 77
Leggett S.K., Allard F., Hauschildt P.H., 1998, ApJ 509, 836
Kirkpatrick J.D., Kelly D.M., Rieke G.H., et al., 1993, ApJ 402, 643
Kirkpatrick J.D., Henry T.J., Simons D.A., 1995, AJ 109, 797
Magazzu A., Martin E.L., Rebolo R., 1993, ApJ 404, L17
Marcy G.W., Lindsay V., Wilson K., 1987, PASP 99, 490
Martin E.L., Basri G., Zapatero Osorio M.R., 1999, AJ 118, 1005
Perryman M.A.C., Lindegren L., Kovalevsky J., et al., 1997, A&A 323, L49
Puxley P.J., Beard S.M., Ramsay S.K., 1992, In: Data analysis workshop. 4th ESO/ST-ECF Garching P. 117
Tinney C.G., Reid I.N., 1998, MNRAS 301, 1031
Tinney C.G., Mould J.R., Reid I.N., 1993, AJ 105, 1045
Tinney C.G., Reid I.N., Gizis J., Mould J.R., 1995, AJ 110, 3014
Tsuji T., Ohnaka K., Aoki W., 1996, A&A 305, 1L
Viti S., Jones H.R.A., Schweitzer A., et al., 1997, MNRAS 291, 780
Wielen R., 1977, A&A 60, 263